RESEARCH ARTICLE

TOPOLOGICAL MATTER

Observation of a Majorana zero mode in a topologically protected edge channel

Berthold Jäck^{1*}, Yonglong Xie^{1*}, Jian Li^{2,3*}, Sangjun Jeon¹ \dagger , B. Andrei Bernevig¹, Ali Yazdani¹ \ddagger

Superconducting proximity pairing in helical edge modes, such as those of topological insulators, is predicted to provide a unique platform for realizing Majorana zero modes (MZMs). We used scanning tunneling microscopy measurements to probe the influence of proximity-induced superconductivity and magnetism on the helical hinge states of bismuth(111) films grown on a superconducting niobium substrate and decorated with magnetic iron clusters. Consistent with model calculations, our measurements revealed the emergence of a localized MZM at the interface between the superconducting helical edge channel and the iron clusters, with a strong magnetization component along the edge. Our experiments also resolve the MZM's spin signature, which distinguishes it from trivial in-gap states that may accidentally occur at zero energy in a superconductor.

ajorana zero modes (MZMs) are non-Abelian quasi-particles that can emerge at the ends of one-dimensional (1D) topological superconductors (1, 2). They may one day provide an experimental setting for topologically protected qubits. To date, strong evidence for the existence of MZMs has come from systems in which the proximity effect from a conventional superconductor is used in concert with strong spin-orbit, Zeeman, or ferromagnetic exchange interaction to engineer a system with topological superconductivity. In particular, experiments on semiconducting nanowires and magnetic atomic chains have provided key signatures of MZMs (3-5) and of their unique charge and spin spectroscopic properties (6-8). However, the presence of MZMs in these platforms does not rely on intrinsically topological electronic states, but rather on engineering 1D band structures with properties suitable for an "effective" p-wave order parameter to emerge when in contact with a conventional s-wave superconductor (9-14). The strength of the induced pairing in these systems, which is the key parameter for the protection of a MZM from quasi-particle poisoning, is also reliant on the strength of spin-orbit interaction.

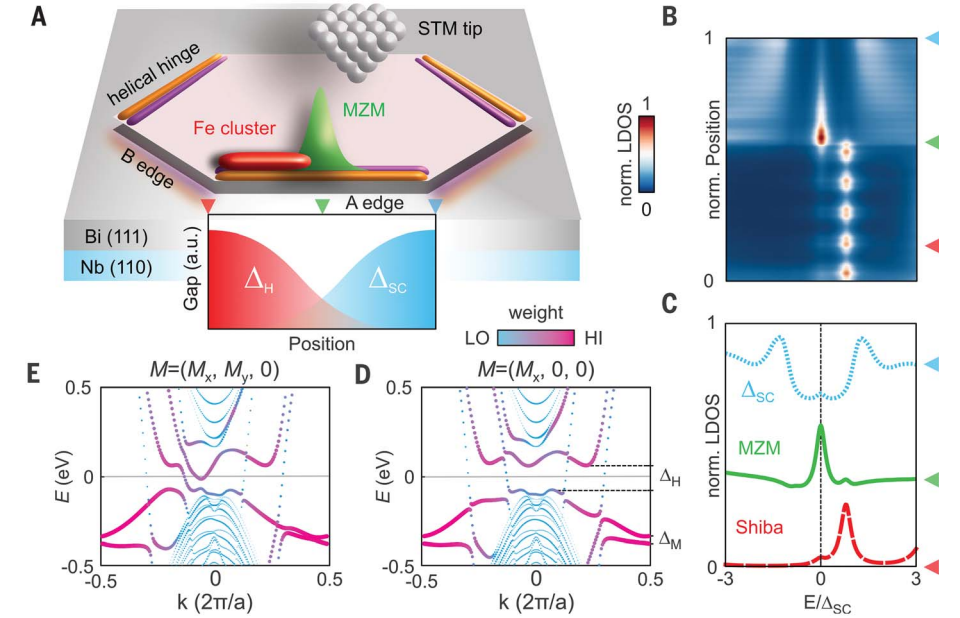
As an alternative to these systems, one might consider topological insulators, the helical edge modes of which intrinsically exhibit large (essentially infinite at low energies in the bulk gap) spin-orbit interaction. Crucially, topological insulators provide a platform where topological superconductivity can be realized in channels that are protected by time reversal symmetry, allowing for material imperfections (15) in the absence of a magnetic field. Because this concept does not rely on band engineering, and because the presence of a magnetic field is not necessary in the superconducting coupled part of the helical edge mode to induce MZMs, the strength of the induced

‡Corresponding author. Email: yazdani@princeton.edu

Fig. 1. Topological superconductivity and Majorana zero modes in the topological edge state of a Bi(111) bilayer. (A) Schematic

representation of a hexagonal Bi bilaver island sitting on the surface of a Bi(111) thin film and exhibiting topological helical states on every other edge. Topological superconductivity Δ_{SC} is induced into these helical states by superconducting proximity from the underlying Nb(110) substrate. Attaching a ferromagnetic cluster to the bilayer edge can open a magnetic hybridization gap Δ_H . A MZM is localized at the mass domain wall, which is realized at the cluster-helical edge state interface, and can be detected in STM experiments. (B) Spatially resolved low-energy LDOS calculated from a tightbinding model for the edge state cluster arrangement shown in (A) (30). The LDOS is a spectroscopic line cut taken along the A edge in (A). (C) Point spectra extracted from the calculated spectroscopic line cut shown in (B) (positions indicated by the colored triangles).

 Γ -M direction from a tight-binding model of a Bi(111) bilayer, for which the A edge is coupled to the spin-polarized d-bands of a ferromagnetic cluster, resulting in a magnetic hybridization gap Δ_H and a Zeeman gap Δ_M . In (D), the cluster magnetization is parallel to the A edge $M=(M_x,0,0)$; in (E), it has an additional component of the same amplitude



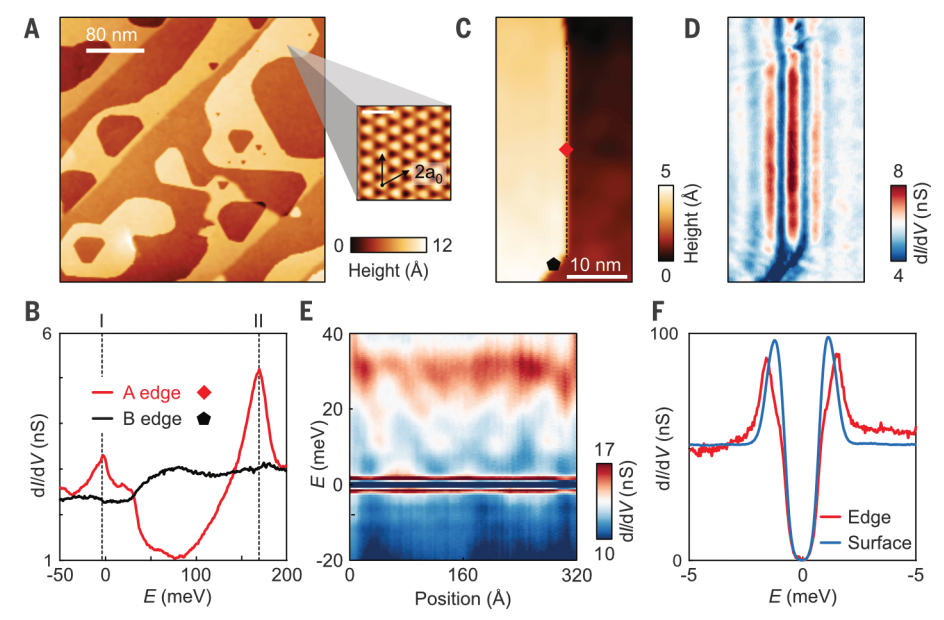
perpendicular to the A edge $M=(M_x,M_y,0)$ (30). The wave function weight on the Bi(111) edge in contact with the cluster is represented by symbol size and position on color scale. The magnetic hybridization gap Δ_H , spanning the entire Brillouin zone, and the Zeeman gap at the high-symmetry point Δ_M are indicated.

(D and E) Calculated band structure along the

¹Joseph Henry Laboratories and Department of Physics, Princeton University, Princeton, NJ 08544, USA. ²Institute for Natural Sciences, Westlake Institute for Advanced Study, Hangzhou, Zhejiang, China. ³School of Science, Westlake University, Hangzhou, China.

^{*}These authors contributed equally to this work. †Present address: Department of Physics, Chung-Ang University, Seoul 06974, Republic of Korea.

Fig. 2. Structural and electronic properties of Bi(111) thin films. (A) Large-scale STM topography of the Bi(111) thin film on Nb(110). Inset: STM topography of the atomic lattice of the surface bilayer together with the lattice vector ao of the hexagonal lattice; scale bar, 1 nm. (B) Point spectra measured on the A edge (red line) and B edge (black line), respectively, at positions indicated in (C). The dashed lines labeled I and II denote energies at which van Hove singularities in the edge state LDOS are observed (set point voltage V_{set} = 200 mV, set point current I_{set} = 2 nA, lock-in oscillation voltage $V_{\text{mod}} = 1 \text{ mV}$). Spatial mapping at these features is demonstrated in (D) and fig. S5. (C) Magnified topography of a typical A edge of a bilayer island, where the A edge is indicated by the red diamond and the B edge by the black pentagon. (D) Spatially resolved dI/dV signal of the sample region shown in (C) ($V_{\text{set}} = 172 \text{ mV}$, $I_{\text{set}} = 2 \text{ nA}$, $V_{\text{mod}} =$ 3 mV). (E) One-dimensional spectroscopic line cut taken along the A edge shown in (C) as indicated by the black dashed line in (C). The



dl/dV signal is plotted as a function of position and energy ($V_{\rm set} = 40$ mV, $I_{\rm set} = 2$ nA, $V_{\rm mod} = 0.3$ mV). (**F**) dl/dV spectra measured in a small energy window around the Fermi energy on the bilayer A edge (red) and on the bilayer surface (blue) ($V_{\rm set} = 5$ mV, $I_{\rm set} = 1$ nA, $V_{\rm mod} = 40$ μ V).

on a Bi(111) surface and a proximity-induced

pairing on such channels could also be large. Thus, relative to existing schemes, this potential MZM platform could provide better protection from both disorder and thermal excitation of quasi-particles (16).

Hinge states as a MZM platform

To realize topological superconductivity and MZMs in a time reversal-protected helical channel, we used the topological edge and hinge states of Bi. Although it has long been recognized that a Bi bilayer in isolation is a 2D topological insulator with 1D helical edge modes (17), recent studies have argued that bulk Bi is an example of a higher-order topological insulator (18-22), which hosts topologically protected 1D helical states along its hinges (23). Consistent with this new perspective, scanning tunneling microscopy (STM) studies on the Bi(111) surface have shown that on the perimeter of a hexagonally shaped bilayer island, every other edge shows signatures of a 1D topological boundary mode (24). This experimental observation can be understood in terms of the hinge modes being hybridized with the surface state of Bi(111) along half of the edges of the hexagonal island (Fig. 1A). Other measurements have also probed Josephson coupling through the Bi hinge states in a nanowire geometry, demonstrating ballistic transport consistent with their topological nature (25). Here, we induced superconductivity in these topological hinge states (26-28) and terminated them using a ferromagnetic cluster, which breaks local time reversal symmetry. The superconductorferromagnetic cluster interface represents a domain wall where the gap changes its character and where we expect a MZM to emerge (Fig. 1A).

Our theoretical consideration of this MZM platform uses a tight-binding model to capture the 1D topological edge states of a bilayer island

pairing on such edge channels via coupling to a conventional bulk superconductor (29); we also account for their hybridization with both the electronic states of a ferromagnetic cluster and those of the underlying Bi bulk, which leads to the hinge-like behavior of these states (30). The results of our theoretical modeling confirm our expectation for the existence of a MZM in the superconducting topological edge states of Bi (Fig. 1). They also show additional features that have not been considered in previous proposals (15, 26) involving topological edge modes, which, however, are important to the experimental implementation. As expected, we find a proximity-induced superconducting gap in the local density of states (LDOS) along the hinge state and a MZM that emerges from this edge channel at the boundary between the regions of dominant induced pairing and magnetic gaps (Fig. 1, A to C). We also find that the hybridization of the hinge states with the Bi bulk states along half of the bilayer edges (Fig. 1A) renders the wave function of the second MZM at the interface with the magnetic cluster highly delocalized, with weak contributions to the LDOS at such locations (30). Our calculation also highlights the presence of in-gap Shiba states, which can occur near magnetic impurities in a superconductor and can appear on the magnetic cluster in the LDOS at finite energy (Fig. 1, B and C) (31, 32). These trivial states require a finite magnetic polarization regardless of its spatial orientation. In contrast, as discussed below, the appearance of a MZM is in addition sensitive to the orientation of the magnetism of the cluster. This difference, as well as differences between the spin properties of the MZM and those of Shiba states, can be used to distinguish a MZM from a trivial zero-energy Shiba state.

Previous proposals considered a local Zeeman interaction for the opening of magnetic gap at the time reversal-invariant points of the topological edge state band structure (15). In our platform, the hybridization of the Bi edge channels with the electronic states of a ferromagnetic cluster (such as Fe in our experiments) results in an additional magnetic hybridization gap $\Delta_{\rm H}$ in the topological edge state band structure (Fig. 1D). Thanks to the direct coupling between the cluster and the edge, a magnetic hybridization gap can have a much larger magnitude than a Zeeman-induced magnetic gap, which enters as a second-order effect in terms of the same coupling. Therefore, in our platform we can circumvent the need for fine-tuning the chemical potential into the magnetic gap for a MZM to emerge. Additional calculations also reveal that the opening of such magnetic hybridization gaps in the proximitized topological band structure is indeed accompanied by a change of the system's topological invariant, as is required for the topological protection of the localized MZM (30). However, as shown in Fig. 1, D and E, the appearance of such a magnetic hybridization gap by coupling the edge mode to the magnetic cluster depends not only on the strength of the coupling, but also on the cluster's magnetic exchange energy scale and the orientation of its magnetization. Although the exact spin polarization of our Bi helical edge mode is not known, we expect the spin polarization to point along some direction orthogonal to the momentum of these 1D states along the edge, similar to other spin momentum-locked topological edge modes. Therefore, a cluster with a magnetization pointing along the edge is most favorable for opening of a gap in the edge state's band structure so as to localize a MZM (Fig. 1D). Additional magnetization components of such clusters modify

the band structure in more complex ways and are usually detrimental to opening up a gap at the Fermi level (Fig. 1E). This sensitivity to the cluster's magnetization shows that MZMs can only emerge for clusters with properly oriented magnetization and ultimately provides the potential ability to turn MZMs on and off on this platform by reorienting the magnetization.

Realization of the platform

To realize our proposed platform, we grew thin films of Bi(111) on a (110)-oriented single crystal of Nb (sputtered and annealed first for cleaning) and used in situ low-temperature STM imaging and spectroscopy at 1.4 K to confirm the presence of topological hinge states on their surface (30). As shown in Fig. 2, these states can be identified on the surface of Bi(111) thin films (thickness 30 Å) by a van Hove singularity in their LDOS, as detected by STM spectroscopy (Fig. 2B) and its mapping (Fig. 2D). They appear on edges we label as type A, where they are not hybridized with the bulk or surface state of Bi crystals. Spectroscopic mapping along finite segments of these edge channels near the Fermi energy shows standing wave patterns in their LDOS (Fig. 2E), the Fourier transform of which reveals the dispersion of a 1D band near the Fermi energy (30). A previous analysis of these standing wave patterns shows that the observed wavelengths are determined by the scattering between nonorthogonal spin states of the edge state band structure within one-half of the Brillouin zone (24). Scattering and interference between time-reversed pairs of states in the edge band structure is not observed in such measurements-a behavior consistent with the absence of backscattering in such topological states.

Owing to the proximity effect from the underlying Nb substrate, superconductivity opens a gap in the 1D band structure at the Fermi energy that can be distinguished from the gap found on the bilayer surface (Fig. 2E). We can separate the gap measured on the A edge into two contributions coming from the surface state and the topological edge state, of which the latter yields a topological gap that can be fitted using Bardeen-Cooper-Schrieffer theory (30). Following this analysis, we find the gap of the topological edge state ($\Delta_T = 1.50 \pm 0.01 \text{ meV}$) to have approximately the same size (in fact, slightly lower; see below) as that measured on the bare Nb(110) substrate surface ($\Delta_S = 1.52 \pm$ 0.01 meV). Given that such superconducting gaps in topologically protected helical channels are intrinsically nontrivial, this system has, by far, the largest gap magnitude as compared to other 1D MZM proximity platforms reported to date, such as atomic chains or semiconductor nanowires, which have $\Delta_{\rm T} \leq$ 200 μeV (4, 5). The application of a magnetic field or the presence of ferromagnetism reduces the p-wave gap considerably in these systems as compared to that of a conventional superconductor used for proximity. One other example of intrinsic topological superconductivity with large gaps (2 meV) has been reported in Fe-based superconductors,

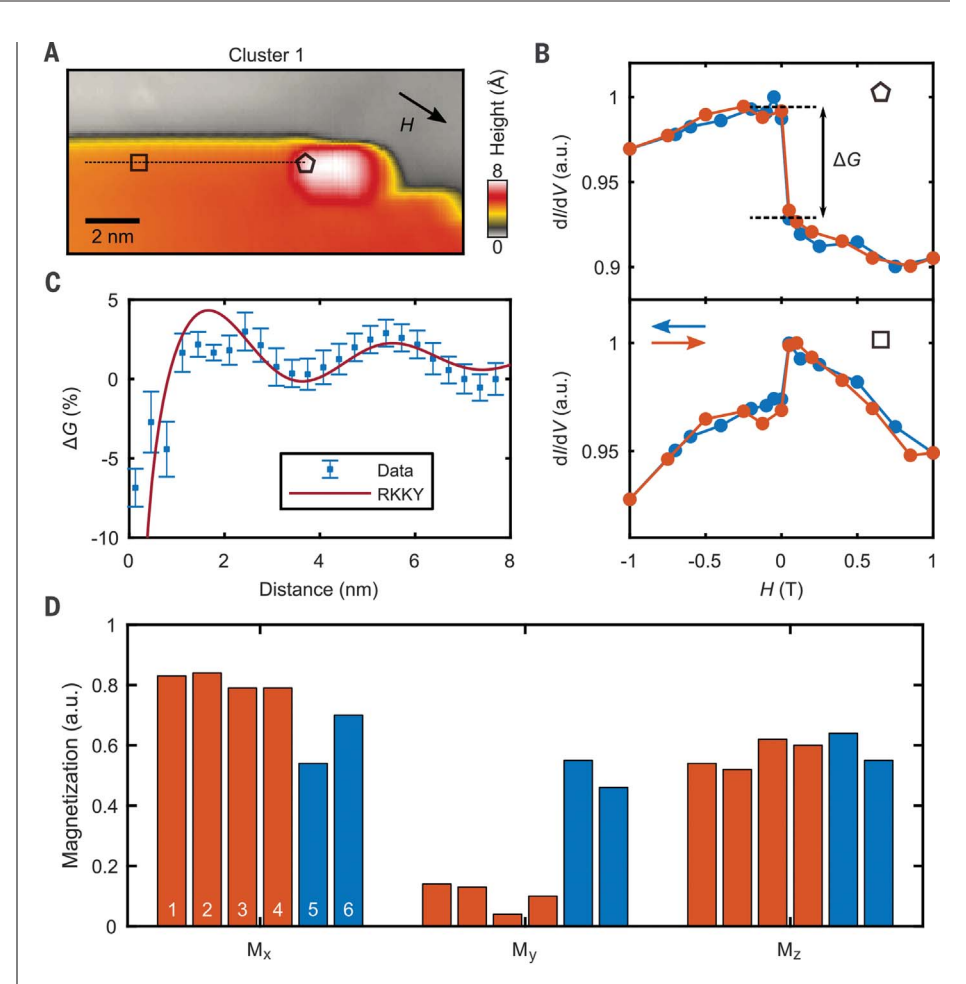


Fig. 3. Spin-polarized measurements on the Fe cluster and the Bi step edge. (**A**) Topography of a Bi step edge decorated with Fe cluster 1. (**B**) Differential tunnel conductance dI/dV measured on the Fe cluster (marked by pentagon) and on the bilayer step edge 6 nm away (marked by square) as a function of the applied magnetic field, the direction of which is indicated in (A). These dI/dV spectra were recorded using a spin-polarized Fe/Cr tip ($V_{\text{set}} = 10 \text{ mV}$, $I_{\text{set}} = 500 \text{ pA}$, $V_{\text{mod}} = 1 \text{ mV}$). (**C**) Spatial dependence of the relative variation of conductance near zero field, ΔG . The burgundy line is a fit using $J_1 - [J_2 \cos(2k_F d)/(2k_F d)]$ (fit parameters: $J_1 = 1.3$, $J_2 = 1.5$, $J_3 = 1.5$,

where signatures of MZMs within the vortex cores of their 2D topological surface states have recently been observed (33, 34).

To introduce a local magnetic perturbation that results in the emergence of MZMs along the proximitized Bi hinge states, we deposited Fe atoms on the Bi(111) surface and annealed the surface (to 373 K), after which we found clusters of Fe nucleated at the bilayer step edges of our sample. The most common location for the nucleation of such clusters was between A and B edges, as shown in Fig. 3. We found some clusters at the center of a B edge (figs. S14 and S15) (30), but we never found clusters at the center of an A edge. The clusters were of different lengths, with a height of 2 to 3 Å (as measured from the top bilayer) in the STM topographies. The magnetic properties of such clusters and their influence on the electronic properties of the topological edge state were characterized by means of spinpolarized STM (30, 35). In such measurements, we recorded the spin-polarized tunnel conductance dI/dV at low bias voltage between the sample and an Fe-coated Cr STM tip as a function of the applied magnetic field. The dI/dVmeasurement on the Fe cluster, hereafter labeled cluster 1, displayed a step-like change of the conductance, ΔG , near zero field, which is characteristic of tunneling between a ferromagnetic cluster and a superparamagnetic tip (Fig. 3B). The small hysteretic behavior in these conductance measurements confirmed the weak magnetic anisotropy of our tip's magnetization and its superparamagnetic behavior. Spin-polarized measurements performed with such tips away from the magnetic cluster along the bilayer A edge also showed similar step-like features in dI/dV. Characterizing these measurements by plotting the relative change of the conductance ΔG with respect to the conductance at small positive magnetic field as a function of the tip distance from the cluster along the A edge (Fig. 3C), we found a behavior indicative of a decaying oscillatory Ruderman-Kittel-Kasuya-Yoshida (RKKY) interaction-induced polarization of the 1D edge state by the Fe cluster (36, 37). The coupling of the Fe clusters to the Bi electronic states appears to also influence the clusters' LDOS, leaving spectroscopic features that can be captured by our model and used to extract the strength of the magnetic hybridization gap in the Bi edge modes caused by the Fe clusters (30). Together, these measurements demonstrate the ferromagnetic nature of the Fe clusters, their ability to induce magnetism into the topological edge state of Bi, and indications of the clusters introducing a sizable magnetic hybridization gap on the Bi edge modes [~80 meV (30)].

Examining different Fe clusters, we observed a similar behavior; however, we also found evidence for variations in the magnetization axis of different clusters. By characterizing STM topographies measured with the superparamagnetic tips that were polarized using our in situ vector magnetic field, we could reconstruct the effective magnetization vector of the clusters (30). Our results for clusters labeled 1 to 6 are summarized in Fig. 3D, showing that these clusters can be separated into two groups (orange and blue) by the amplitude of their magnetization

component perpendicular to the edge. Such different cluster magnetizations may affect the 1D edge modes' band structure in multiple ways, as anticipated by our model calculations shown in Fig. 1 (30).

Observation of MZMs

Having established the presence of both superconducting pairing and ferromagnetism in our samples, we used high-resolution STM spectroscopy to probe the low-energy properties and to search for localized MZMs in this system. In Fig. 4, we show a typical example of such an experiment on cluster 2 that reveals the emergence of a sharp zero-bias peak (ZBP) within the pairing gap along the Bi bilayer A edge (peak width $\Delta E \leq 400 \mu eV$; Fig. 1, B to D) as the tip approaches the hinge-cluster interface. Spectroscopy on top of the cluster, away from the interface, shows Shiba states at finite positive and negative energies that are separated by a suppression of the tunnel conductance at zero energy (Fig. 1, B and C). A detailed analysis of the spatial profile of the ZBP in Fig. 4D demonstrates that it is strongest in magnitude on the superconducting 1D channel, precisely at the interface of the channel with the Fe cluster. The tail of the ZBP extends along the channel and, as shown in Fig. 4D, can still be detected at about half of its peak value 2 nm away from the

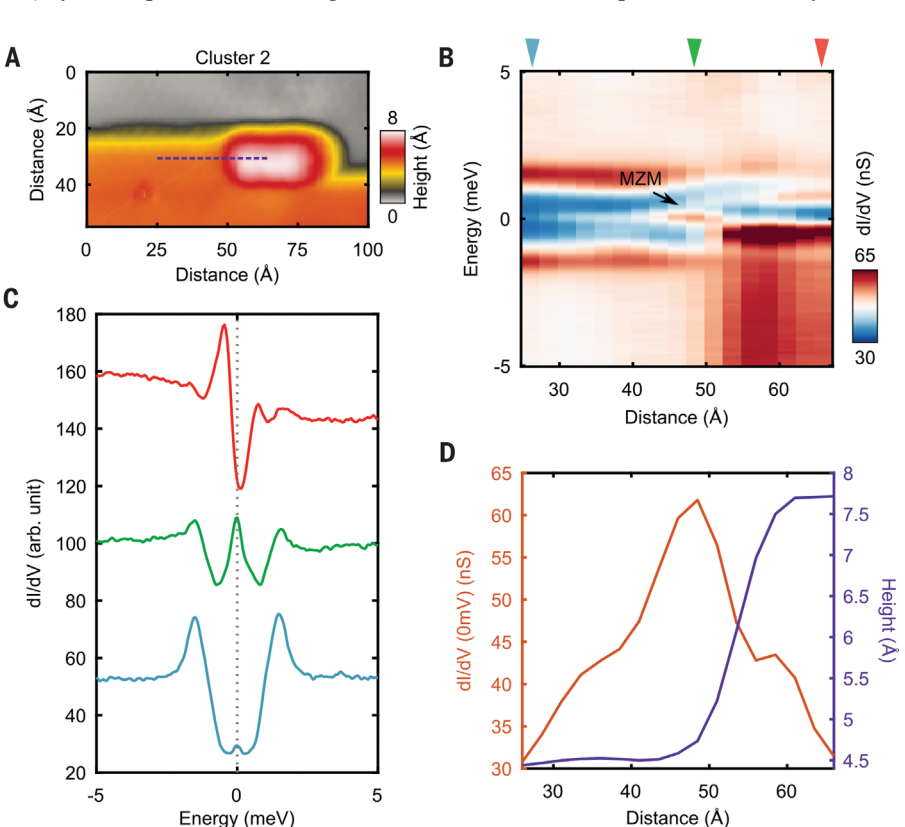


Fig. 4. Localized ZBP at the interface. (**A**) Topography of a Bi step edge decorated with Fe cluster 2. (**B**) Spectroscopic line cut taken along the purple dashed line in (A) ($V_{\text{set}} = 5 \text{ mV}$, $I_{\text{set}} = 1 \text{ nA}$, $V_{\text{mod}} = 40 \, \mu\text{V}$). (**C**) Individual point spectra at locations indicated by triangular markers in (B). For clarity, the spectra are offset from each other by 45 nS. (**D**) Simultaneously measured tunnel conductance dl/dV at zero energy (red) and topographic height (purple) along the purple dashed line in (A).

interface. This length scale is consistent with the theoretical expectation of the spatial decay of the MZM wave function in our system, when we crucially take into account the renormalization of the edge mode Fermi velocity caused by the proximity effect with the Nb substrate (30, 38–40). We also observed the presence of such a ZBP localized at the hinge-cluster interface for clusters 1, 3, and 4 (fig. S11) (30). Overall, our experimental observation of a localized ZBP in these experiments is consistent with our model calculations described in Fig. 1 and with the interpretation of the ZBP as a spectroscopic signature of a MZM.

Examining other clusters under varying experimental conditions, we obtained further observations that corroborate the interpretation of the ZBP as due to the presence of a MZM (30). We found that the ZBP is absent when the application of a magnetic field suppresses superconductivity in our hybrid system, thereby excluding the Kondo effect as the origin of the ZBP (fig. S13). We also found that Fe clusters on top of B edges, where the edge modes are strongly hybridized with the bulk states, do not show ZBPs, suggesting that the presence of an isolated helical edge mode is required for the ZBP to appear (fig. S14). The data on these edges also demonstrate that the Fe clusters, even those as long as 80 Å, are not the source of the ZBP themselves (fig. S15). This is in contrast to other magnetic atomic chain systems on the surface of a superconductor (4), for which a nontrivial bulk topology of the chain itself can induce topological superconductivity and localize MZMs. Our theoretical modeling also predicts a second weakly localized MZM at the interface between an Fe cluster and a B edge owing to the hybridization of the topological edge state with the underlying bulk states on the B edge. Spectroscopic measurements near the B edge found signatures of an LDOS enhancement near zero energy consistent with this prediction (30). More important, although our observation of a ZBP has been reproduced for many superconducting A edge-Fe cluster interfaces (30), a fraction of these systems did not show a ZBP. When comparing with the reconstructed magnetization vectors of the different Fe clusters shown in Fig. 3D, we observe a clear correlation between the observation of a ZBP and the type of cluster magnetization. Clusters 1 to 4 have a weak magnetization component perpendicular to the edge and show a ZBP, whereas clusters 5 and 6 have a sizable magnetization component perpendicular to the edge and do not show a ZBP. Such behavior is consistent with our model calculations (Fig. 1E) (30), which show that a magnetization component perpendicular to the edge is detrimental to inducing the magnetic hybridization gap in the topological edge state necessary to localize a MZM.

Spin polarization of MZMs

Finally, we used energy-resolved spin-polarized spectroscopic measurements with the STM to

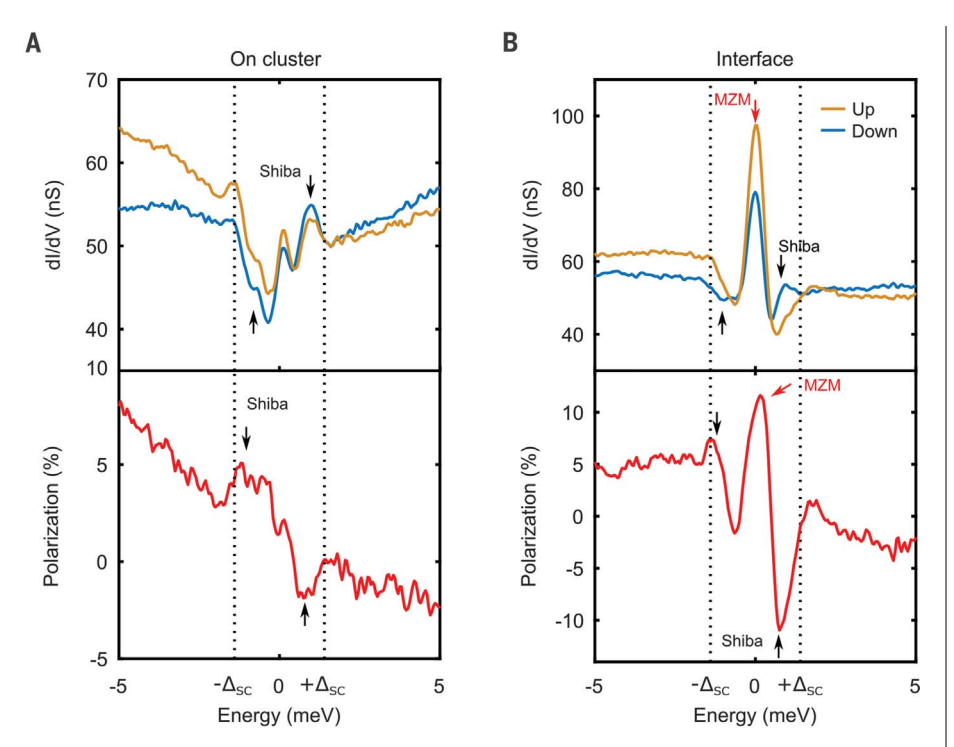


Fig. 5. Spin polarization of MZM and Shiba states. (A and B) dl/dV spectra on the Fe cluster (A) and at the interface (B) as well as their corresponding spin polarizations ($V_{\text{set}} = -5 \text{ mV}$, $I_{\text{set}} = 1 \text{ nA}$, $V_{\text{mod}} = 1 \text{ nA}$ 40 μV). Yellow and blue curves are taken with "up"- and "down"-polarized tips, respectively. Red arrows mark the zero-bias end state; black arrows mark the van Hove singularity of the Shiba band.

demonstrate that we can distinguish the presence of a MZM from that of a trivial zero mode, which might form accidentally in our system. Previous studies have shown that trivial in-gap states appear with an energy-asymmetric characteristic in the extracted spin polarization P(E)from spin-resolved STM spectroscopic measurements under constant-current conditions (6, 40). When we carried out such measurements on the Fe clusters, we found the predicted behavior of P(E) for the Shiba states induced at low energies by these clusters (Fig. 5A). This asymmetric behavior of trivial states in P(E) results in their lacking spin contrast in this measurement at zero energy, and thereby can be used as a diagnostic tool to distinguish MZMs. As shown in Fig. 5B, the ZBP at the A edge-Fe cluster interface shows a strong spin contrast at zero energy, hence confirming that it does not arise from a trivial zero-energy mode. Besides this important distinction between the MZM and trivial Shiba states, fundamentally in our platform the magnetizations of these two different states are expected to point along different orientations. The spin orientation of the Shiba states is dictated by the orientation of the magnetic cluster, whereas the MZM occurring in the topological channel generically has a different spin orientation, which can even be perpendicular to the Shiba state (30). The differing sign of the spin polarization P(E) of the MZM and the positive-energy Shiba state is consistent with this expectation and adds yet another unique feature of the MZM formed at the interface between

superconductivity and magnetism on a topological edge mode (30).

Looking ahead, our demonstration of MZMs within the topological edge states of Bi can be extended to Bi nanowires (25) and similar realization in other 2D or 3D higher-order topological insulators by using magnetic clusters as a way of localizing MZMs in the presence of proximityinduced superconductivity. The Bi nanowires also provide a viable approach to creating devices based on this platform. Clusters with weak magnetic anisotropy could be used to turn on and off the MZMs with in-plane magnetic fields reliably. If such fields are low enough, they might be able to switch the magnetic state of the clusters without disrupting the superconductivity of the edge. The use of spin-torque tunneling effects can present a viable alternative to switch the cluster magnetization, thereby providing an approach to manipulate the presence of MZMs. In view of the recent progress in the field of 2D materials (41-43), we anticipate that this approach of localizing MZMs in topologically protected helical edge channels may also be realized using van der Waals heterostructures.

REFERENCES AND NOTES

- 1. A. Y. Kitaev, Ann. Phys. 303, 2-30 (2003).
- C. Nayak, S. H. Simon, A. Stern, M. Freedman, S. Das Sarma, Rev. Mod. Phys. 80, 1083-1159 (2008).
- V. Mourik et al., Science 336, 1003-1007 (2012).
- S. Nadj-Perge et al., Science 346, 602-607 (2014).
- M. T. Deng et al., Science 354, 1557-1562 (2016).
- S. Jeon et al., Science 358, 772-776 (2017).
- F. Nichele et al., Phys. Rev. Lett. 119, 136803 (2017).
- H. Zhang et al., Nature 556, 74-79 (2018).

- A. Y. Kitaev, Phys. Uspekhi 44, 131-136 (2001).
- 10. R. M. Lutchyn, J. D. Sau, S. Das Sarma, Phys. Rev. Lett. 105, 077001 (2010)
- Y. Oreg, G. Refael, F. von Oppen, *Phys. Rev. Lett.* **105**, 177002 (2010). S. Nadj-Perge, I. K. Drozdov, B. A. Bernevig, A. Yazdani, Phys. Rev. B 88, 020407 (2013).
- F. Pientka, L. I. Glazman, F. von Oppen, Phys. Rev. B 88, 155420 (2013).
- 14. J. Klinovaja, P. Stano, A. Yazdani, D. Loss, Phys. Rev. Lett. 111, 186805 (2013).
- L. Fu, C. L. Kane, Phys. Rev. B 79, 161408 (2009)
- D. Rainis, D. Loss, *Phys. Rev. B* **85**, 174533 (2012) S. Murakami, *Phys. Rev. Lett.* **97**, 236805 (2006).
- 17.
- W. A. Benalcazar, B. A. Bernevig, T. L. Hughes, Science 357, 61-66 (2017).
- W. A. Benalcazar, B. A. Bernevig, T. L. Hughes, Phys. Rev. B 96,
- J. Langbehn, Y. Peng, L. Trifunovic, F. von Oppen,
- P. W. Brouwer, Phys. Rev. Lett. 119, 246401 (2017)
- 21. Z. Song, Z. Fang, C. Fang, Phys. Rev. Lett. 119, 246402 (2017).
- 22. F. Schindler et al., Sci. Adv. 4, eaat0346 (2018).
- 23. F. Schindler et al., Nat. Phys. 14, 918-924 (2018)
- 24. I. K. Drozdov et al., Nat. Phys. 10, 664-669 (2014)
- 25. A. Murani et al., Nat. Commun. 8, 15941 (2017).
- 26. S. Mi, D. I. Pikulin, M. Wimmer, C. W. J. Beenakker, Phys. Rev. B 87. 241405 (2013).
- C. H. Hsu, P. Stano, J. Klinovaja, D. Loss, Phys. Rev. Lett. 121, 196801 (2018).
- 28. R. Queiroz, A. Stern, arXiv:1807.04141 [cond-mat.mes-hall] (1 March 2019)
- 29. H.-H. Sun et al., Nano Lett. 17, 3035-3039 (2017)
- 30. See supplementary materials
- 31. A. Yazdani, B. A. Jones, C. P. Lutz, M. F. Crommie, D. M. Eigler, Science 275, 1767-1770 (1997).
- 32. A. V. Balatsky, I. Vekhter, J.-X. Zhu, Rev. Mod. Phys. 78, 373-433 (2006).
- 33. D. Wang et al., Science 362, 333-335 (2018).
- 34. T. Machida, Y. Sun, S. Pyon, S. Takeda, Y. Kohsaka, T. Hanaguri, T. Sasagawa, T. Tamegai, arXiv:1812.08995 [cond-mat.supr-con] (25 December 2018).
- 35. R. Wiesendanger, Rev. Mod. Phys. 81, 1495-1550 (2009).
- 36. J. M. D. Coey, in Magnetism and Magnetic Materials (Cambridge Univ. Press, 2009), pp. 141-143.
- 37. F. Meier, L. Zhou, J. Wiebe, R. Wiesendanger, Science 320, 82-86 (2008).
- 38. T. D. Stanescu, R. M. Lutchyn, S. Das Sarma, Phys. Rev. B 84, 144522 (2011).
- 39. Y. Peng, F. Pientka, L. I. Glazman, F. von Oppen, Phys. Rev. Lett. 114, 106801 (2015).
- 40. J. Li, S. Jeon, Y. Xie, A. Yazdani, B. A. Bernevig, Phys. Rev. B 97, 125119 (2018)
- 41. S. Wu et al., Science 359, 76-79 (2018).
- 42. V. Fatemi et al., Science 362, 926-929 (2018).
- 43. B. Huang et al., Nature 546, 270-273 (2017).
- 44. B. Jäck et al., Replication data and theory code for: Observation of a Majorana zero mode in a topologically protected edge channel, http://dx.doi.org/10.5281/zenodo.2779382 (2019).

ACKNOWLEDGMENTS

We thank A. Johansson for initial theoretical support. Funding: Supported by the Gordon and Betty Moore Foundation as part of the EPiQS initiative (GBMF4530), ONR-N00014-17-1-2784, ONR-N00014-14-1-0330, NSF-MRSEC programs through the Princeton Center for Complex Materials DMR-1420541, and NSF-DMR-1608848. Also supported by the Alexander von Humboldt Foundation through a Feodor-Lynen postdoctoral fellowship (B.J.): DOE de-sc0016239, NSF EAGER 1643312, Simons Investigator Grants, ARO MURI W911NF-12-1-0461, the Packard Foundation, and the Schmidt Fund for Innovative Research (B.A.B.); and the National Natural Science Foundation of China under project 11774317 (J.L.). The calculations of band structures and density of states in this work were supported by U.S. Department of Energy grant DE-SC0016239. Author contributions: B.J., Y.X., S.J., and A.Y. designed and conducted the experiment; B.J., Y.X., and A.Y. analyzed the data; B.J., J.L., and B.A.B. performed the theoretical calculations; and all authors contributed to the writing of the manuscript. Competing interests: The authors declare no competing interest. Data and materials availability: The experimental data

SUPPLEMENTARY MATERIALS

science.sciencemag.org/content/364/6447/1255/suppl/DC1 Materials and Methods

and theory code of this study are available at (44).

Figs. S1 to S15

Tables S1 and S2 References (45-47)

25 February 2019; accepted 4 June 2019

Published online 13 June 2019

10.1126/science.aax1444



Observation of a Majorana zero mode in a topologically protected edge channel

Berthold Jäck, Yonglong Xie, Jian Li, Sangjun Jeon, B. Andrei Bernevig and Ali Yazdani

Science 364 (6447), 1255-1259.

DOI: 10.1126/science.aax1444originally published online June 13, 2019

Majorana on a hinge

One of the early proposals for the physical implementation of Majorana zero modes (MZMs) centered on inducing superconductivity in a topological insulator (TI) by placing it in contact with a superconductor. Jäck *et al.* used scanning tunneling spectroscopy to observe MZMs in a similar heterostructure. In their devices, the TI is a hexagonal bismuth island placed on top of a layer of superconducting niobium. The bismuth island had topological boundary hinge states on every other edge of the hexagon. Placing a cluster of iron atoms on the hinge generated a zero-bias peak characteristic of MZMs at the interface between the cluster and the hinge state.

Science, this issue p. 1255

ARTICLE TOOLS http://science.sciencemag.org/content/364/6447/1255

SUPPLEMENTARY http://science.sciencemag.org/content/suppl/2019/06/12/science.aax1444.DC1

REFERENCES This article cites 46 articles, 12 of which you can access for free

http://science.sciencemag.org/content/364/6447/1255#BIBL

PERMISSIONS http://www.sciencemag.org/help/reprints-and-permissions

Use of this article is subject to the Terms of Service